

Atomistic simulation studies on the effect of pressure on diffusion at the MgO 410/[001] tilt grain boundary

Duncan J. Harris

Department of Geological Sciences, University College London, Gower Street, London WC1E 6BT, United Kingdom

Graeme W. Watson

Department of Chemistry, Trinity College, Dublin 2, Ireland

Stephen C. Parker

*Department of Chemistry, University of Bath, Claverton Down, Bath BA2 7AY, United Kingdom**

(Received 2 April 2001; published 31 August 2001)

We have used atomistic simulation techniques to examine the effect of pressure on atom transport in the 410/[001] tilt grain boundary of MgO. The approach was to compare the diffusion pathways and migration energies for cation and anion vacancy migration at 0 and 40 GPa. The effect of pressure was to increase the migration energies and to increase the preference for vacancies to reside at the boundary rather than at bulk lattice sites. Furthermore, if present in any significant concentration, the vacancies will be bound and remain bound during diffusion, which results in the migration energies being similar to those found for diffusion in the bulk. Hence the results suggest that, as expected, the boundary has higher diffusivities than the bulk but that this is a result of the larger number of mobile species rather than lower migration energies.

DOI: 10.1103/PhysRevB.64.134101

PACS number(s): 68.35.Fx, 64.70.Kb

I. INTRODUCTION

Atomic transport in ceramic polycrystalline solids is often dominated by diffusion at the grain boundaries, and thus it is important to study these boundaries, preferably at the atomic level. A great deal of experimental work has been carried out on polycrystalline materials at ambient conditions.¹⁻⁴ Atkinson and co-workers^{5,6} measured NiO grain boundary diffusion and showed that the activation energy for vacancy migration was significantly lower along the boundary than in single crystal NiO. In contrast, Wuensch and Tuller⁷ measured the rates of diffusion of Ni²⁺ in ZnO and found that although enhancement of the diffusion did occur at the grain boundary the activation energy for this process was much the same as that for bulk. They attributed the enhanced diffusion to the higher defect concentrations that were found at the boundary. Both of these experiments demonstrate enhanced diffusion at the grain boundary; however, they disagree on the mechanism that causes this enhancement. Atomistic simulation gives us the opportunity to investigate both mechanisms by calculating the activation energy for atom migration and the defect concentrations in both the bulk and at a grain boundary. Furthermore, the use of atomistic simulation techniques allows different conditions to be investigated, such as the effect of pressure on atom migration, which is difficult to study experimentally. Indeed, there has been little experimental study of the effect of pressure on diffusion at grain boundaries. Some work does exist for metals; for example, experiments on indium diffusion in copper bicrystals showed an increase in the diffusion coefficient with increasing pressure up to 1 GPa.⁸ In the area of ceramics, Stubican and Carinci⁹ performed diffusion experiments on NiO and Fe₃O₄ at various oxygen pressures up to 1 MPa and found that the diffusion coefficient increased with in-

creasing pressure. In this work we have considered higher pressures such as would be found in geophysical processes.

We have chosen to use atomistic simulation techniques that employ potential models to describe the interatomic forces rather than use a full electronic structure calculation, simply because the atomistic approach can treat a much larger number of atoms. The large simulation cells are necessary when studying migration along grain boundaries, but one must have confidence in the potential model describing the interatomic forces. In the case of MgO there is much evidence that the models are reliable and this is one of the reasons for choosing MgO as our first system. One recent example by Harding and Noguera¹⁰ showed that the calculated structure and energy of a (100) twist grain boundary in MgO from atomistic and electronic structure techniques were virtually identical. Although there has been a good body of atomistic simulation work on bulk minerals there has been considerably less on diffusion at oxide or mineral grain boundaries. Duffy and Tasker¹¹ used atomistic simulation to calculate the activation energy for cation vacancy hopping in the {310}/[001] symmetric tilt grain boundary of NiO and found that the activation energy was lower than that for bulk. A similar result was found by Meyer *et al.*¹² using molecular dynamics. We have previously investigated the self-diffusion pathways in the MgO {410}/[001] grain boundary at 0 GPa,¹³ the details of which will be discussed later.

In this paper we present the results of atomistic simulations to calculate the effect of pressure upon the diffusion pathways and migration energies of vacancies at the {410}/[001] tilt grain boundary of MgO. MgO was chosen because it is a simple face-centered cubic crystal and, as noted above, has a reliable potential model. Furthermore, the effect of pressure was modeled by comparing the activation energies for diffusion at 0 GPa with the activation energies at 40 GPa. This high pressure was chosen so that the effects of pressure

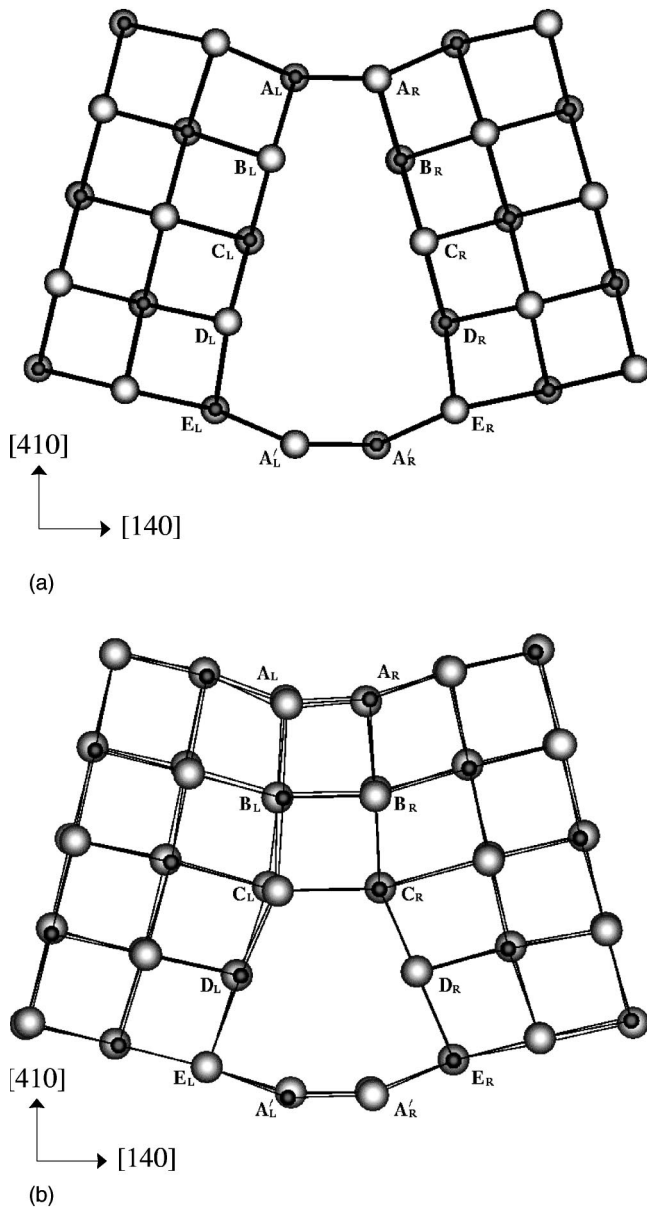


FIG. 1. Relaxed structure of the $\{410\}/[001]$ tilt grain boundary of MgO at (a) 0 GPa and (b) 40 GPa showing how the dislocation pipes collapse with pressure. The letters indicate unique vacancy sites along the boundary.

could be clearly seen and, as MgO is a significant component of the lower mantle that can experience these pressures, the results have relevance to those studying transport processes in the lower mantle. The grain boundary is formed by the rotation of two blocks of bulk MgO crystal about the $[001]$ axis. Surfaces are created from each block, and when these are joined together they form a series of dislocation pipes at the boundary [Fig. 1(a)]. The boundary was chosen so that we could compare the results with those previously obtained from simulations performed on the boundary when no pressure is applied. We have previously shown¹⁴ that the $\{410\}$ tilt boundary of MgO undergoes a structural transition at high pressure to form a more compact structure [Fig. 1(b)] that may significantly affect the diffusion process. Further

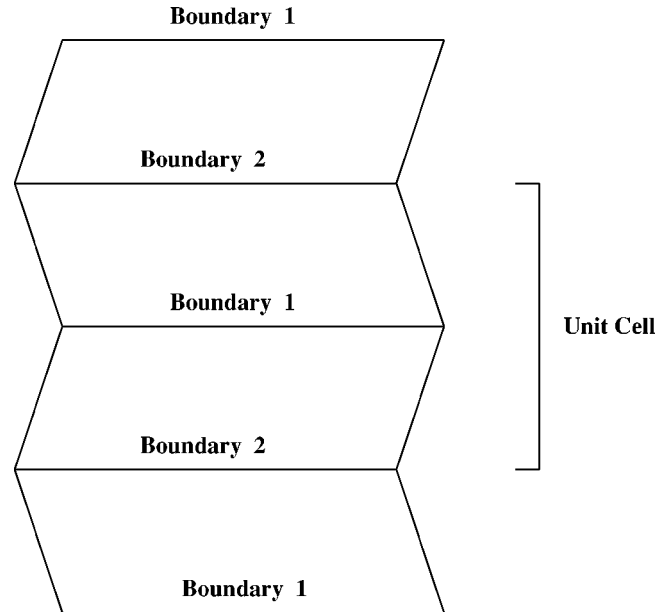


FIG. 2. Schematic diagram of the construction of a three-dimensional periodic unit cell containing a grain boundary.

work has shown that this compressed structure is stable up to approximately 60 GPa before a further structural transition occurs.¹⁵

II. COMPUTATIONAL METHODS

We generated the grain boundary simulation cell by creating a unit cell from the two oriented blocks that formed the interface. First the two blocks of crystal, one terminating in (410) surface and the other expressing the (410) surface were brought together. The unit cell was created by repeating the two oriented blocks in three dimensions leading to a simulation cell containing two grain boundaries, one in the center of the unit cell and the second at the point where two cells meet (Fig. 2). The cell contained 960 atoms to make it large enough to minimize interactions between the boundaries. Energy minimization calculations were performed to calculate the energies of forming oxygen and magnesium vacancies both in the boundary and in bulk MgO and to provide starting configurations for our simulations.

The computer simulations are based on the Born model of ionic solids in which the forces between the ions are modeled by summation of pairwise interatomic potentials. In this study we have used the potential model of Lewis and Catlow¹⁶ that includes Coulombic and short range interactions. Normally this type of potential model also includes the shell model¹⁷ to simulate the electronic polarizability of the ions. However, we have removed the shells and considered only rigid ions because of the large amount of computer time required for this study. A formal estimate of the error resulting from the use of the rigid ion approximation is difficult to quantify. However, one approach is to compare the calculated vacancy formation energies at the grain boundary using rigid ion and shell models. The use of the rigid ion approximation does cause the formation energies to be overesti-

TABLE I. Cation partial Schottky energies (PSE) for the {410} tilt grain boundary of MgO at 40 GPa and 0 GPa data (Harris *et al.*, Ref. 13) and the energies relative to the bulk formation energy. A negative energy corresponds to a preference in forming a vacancy relative to the bulk.

| Vacancy position (type) | Partial Schottky energy (eV) | | PSE relative to bulk vacancy (eV) | |
|-------------------------|------------------------------|--------|-----------------------------------|--------|
| | 0 GPa | 40 GPa | 0 GPa | 40 GPa |
| A (Mg) | 3.53 | 2.43 | -0.63 | -2.49 |
| B (Mg) | 4.11 | 3.67 | -0.05 | -1.25 |
| C (Mg) | 4.21 | 4.73 | +0.05 | -0.19 |
| D (Mg) | 3.69 | 2.43 | -0.47 | -2.49 |
| E (Mg) | 4.99 | 5.32 | +0.83 | +0.40 |
| Bulk (Mg) | 4.16 | 4.92 | - | - |
| A (O) | 3.97 | 3.08 | -0.65 | -2.39 |
| B (O) | 4.44 | 4.16 | -0.18 | -1.31 |
| C (O) | 4.59 | 5.23 | -0.03 | -0.24 |
| D (O) | 4.05 | 3.08 | -0.57 | -2.39 |
| E (O) | 5.34 | 5.80 | +0.72 | +0.33 |
| Bulk (O) | 4.62 | 5.47 | - | - |

mated by a few tenths of an eV compared to the shell model, but does not change the relative stabilities of the sites.¹³ Hence, there should not be any significant differences between the two models. Furthermore, we are considering migration energies, which are relative energies, and so it is likely that a large part of the error is cancelled, at least in the case of MgO.

The energies required to form the vacancies were calculated using both energy minimization and traditional molecular dynamics (MD). The MD approach directly solves Newton's laws of motion over a finite time span for a periodically repeating box of ions. The Nosé-Hoover constant temperature method^{18,19} places the cell in contact with a heat bath, allowing energy to transfer into or out of the cell ensuring that a constant temperature ensemble is obtained. Initially the ions are assigned random velocities such that the system starts out with the desired simulation temperature. The MD proceeds by using the forces calculated from a potential model to update the velocity and position of the ions by solving Newton's laws of motion numerically, in our case using a fifth-order predict corrector method due to Gear.²⁰

The energetics associated with diffusion can then be evaluated. There are two components: the first is the energy to form the defect and the second is the migration or activation energy. However, the difficulty in using traditional MD to model diffusion in oxides is that the migration energies for ion migration are often much greater than the thermal energy available. Thus, very high temperatures or extremely long run times must be used to calculate migration energies and diffusion pathways of the slower moving species as demonstrated by Meyer *et al.*¹² Often the temperature employed is close to the melting point of the material. To overcome this problem we modified our MD code^{21,22} to calculate diffusion pathways and migration energies directly.¹³

The approach was to place a single vacancy into a simulation cell of 960 ions that had previously been obtained from a MD run at 40 GPa within the isothermal, isobaric ensemble (*NPT*). A small force was added to the moving ion

each step to ensure that the net force on the moving ion always contained a small component in the direction of the vacancy. This caused it to move slowly towards the vacancy whilst allowing motion perpendicular to the direction of diffusion. This is essential because both Duffy and Tasker¹¹ in NiO and Vocadlo *et al.*²⁴ in bulk MgO showed that the migration path was not always linear between the two lattice sites. A counter force of equal magnitude but in the opposite direction was added to the remaining ions to ensure the cell had no net translational momentum. In addition, the volume was kept constant at the volume obtained from the MD simulation obtained under *NPT* conditions, and the velocities of the ions were scaled each step to ensure that no net energy was added to the system from the applied forces. The temperature was set at 10 K to allow the rest of the crystal to relax as the ion moved from one site to another.

III. RESULTS

The calculated {410} tilt grain boundary has a structure consisting of a series of dislocation pipes. Several sites are available for vacancy formation at the boundary, as shown in Fig. 1(b) where *L* and *R* are used to distinguish similar sites to the left and right of the boundary. It should be noted that positions *A* and *A'* on the figure legend are equivalent sites. Since we are interested in comparing the energies of forming single vacancies, we have defined the ‘‘partial Schottky energy’’ as the energy to remove a single ion and place into a bulk lattice site. Although the partial Schottky energies are not measurable experimentally they are useful for comparing relative site stabilities. Table I lists the calculated partial Schottky energies for sites at the grain boundary, labeled in Fig. 1(b), at 40 GPa and compares them to the energies calculated previously at 0 GPa.¹³ The relative energies show that the vacancy becomes more stable at the boundary compared to the bulk for each vacancy site as the pressure is

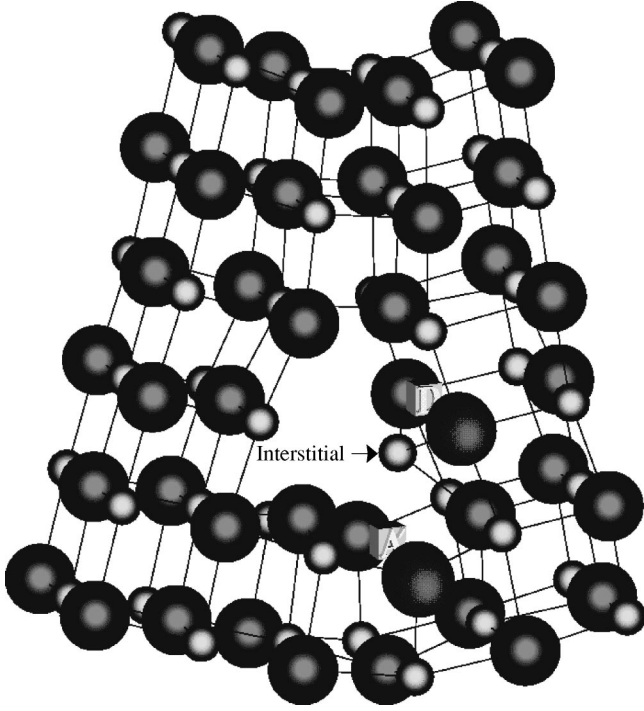


FIG. 3. Structure of the $\{410\}$ boundary at 40 GPa. The vacancy sites of D and A' are highlighted. The ion in the interstitial position between these sites is the energetically most favorable position of the ion, rather than in one of the vacant sites.

increased. This causes site C , which was less stable than the bulk at 0 GPa, to become more stable. Site E still remained the least stable site.

The A and D sites were the most energetically preferred sites for vacancies with a partial Schottky energy of less than half of that of the bulk. Examination of the boundary structure after relaxation with a vacancy at either the A or D sites revealed them to be identical. The reason was that the relaxation caused the ion at the site not containing the vacancy to be moved into an interstitial position between the two sites, thus giving rise to the identical structures (Fig. 3). A similar effect did not occur for the boundary at 0 GPa because at 0 GPa the sites, A and D , are quite distant but at high pressure the more compact boundary structure results in sites A and D being brought closer together. Moreover, in the 0 GPa simulation the central position between sites A and D was at an energy maximum and not an energy minimum.

The lowering of the defect energies for the most stable site suggests that the concentration of defects at the boundary will increase relative to the 0 GPa case. We followed the work of Duffy and Tasker²⁵ to calculate relative concentrations of vacancies at the boundary relative to the bulk including a treatment of the space charge in the region of the vacancies.

For a bulk crystal with N available sites for vacancy formation, the number of bulk sites occupied (n_0) is given by

$$\frac{n_0}{N} = \exp\left[-\left(\frac{F^{\text{Mg}} + F^{\text{O}}}{2kT}\right)\right] \quad (1)$$

where F^{Mg} and F^{O} are the partial Schottky energies in the bulk, k is the Boltzmann constant, and T is the temperature. For the boundary with N_b sites, the fraction of sites occupied (n_b) is given by

$$\frac{n_b}{N_b} = \left(\frac{n_0}{N}\right) \exp\left[-\left(\frac{F_I^{\text{Mg}} + F_I^{\text{O}}}{2kT}\right)\right] (1 + \delta) \quad (2)$$

where $F_I^{\text{Mg}} = F_B^{\text{Mg}} - F^{\text{Mg}}$ and $F_I^{\text{O}} = F_B^{\text{O}} - F^{\text{O}}$ (F_B^{Mg} and F_B^{O} are the boundary partial Schottky energies) and δ is given by

$$\delta = \frac{\left[2\kappa^{-1} \left(\frac{n_b}{N_b}\right) \exp\left(\frac{F_I^{\text{Mg}}}{2kT}\right) \sinh\left(\frac{F_I^{\text{Mg}} - F_I^{\text{O}}}{4kT}\right)\right]}{\left[1 + \kappa^{-1} \left(\frac{n_b}{N_b}\right) \exp\left(\frac{F_I^{\text{Mg}} + F_I^{\text{O}}}{2kT}\right) \cosh\left(\frac{F_I^{\text{Mg}} - F_I^{\text{O}}}{4kT}\right)\right]}, \quad (3)$$

where the screening length κ^{-1} is given by

$$\kappa^{-1} = \left(\frac{\epsilon_0 \epsilon kT}{2e^2 n_0}\right)^{1/2}, \quad (4)$$

where ϵ_0 is the permittivity of a vacuum, ϵ is the permittivity of the material, and e is the electronic charge.

Bulk MgO has $5.4 \times 10^{28} \text{ m}^{-3}$ available sites, N , and for the boundary we are considering N_b to be $2.7 \times 10^{18} \text{ m}^{-2}$. The use of the space charge equation noted above gives a ratio for the fraction of boundary to bulk sites occupied by vacancies at 1500 K and 40 GPa pressure of 4.3×10^7 , which can be compared to 11.4 calculated for 0 GPa at 1500 K. Thus the effect of pressure is shown clearly to increase the vacancy concentrations at the boundary. We therefore suggest at these high pressures there is apparently a $10^6 - 10^7$ enhancement in grain boundary migration relative to the bulk, simply from the relative increase in numbers of mobile species. However, we need also to examine the effect of pressure on migration energy, which is discussed in the next section.

A. Diffusion path for isolated vacancies

Initially the modified MD code was used to evaluate the migration energy of single vacancies in the bulk crystal. The calculated energies for magnesium and oxygen vacancy migration were $2.68 \pm 0.1 \text{ eV}$ and $2.58 \pm 0.1 \text{ eV}$, respectively, at 40 GPa and as expected are greater than the 0 GPa values of $1.94 \pm 0.1 \text{ eV}$ and $2.12 \pm 0.1 \text{ eV}$, simply due to the 9% reduction of the lattice parameter. Vocadlo *et al.*²⁴ also calculated the migration energy at 0 GPa, but using lattice dynamics rather than MD. They obtained values of 1.99 and 2.00 eV, respectively, which agree within the uncertainties of the results. Note that the migration energy for oxygen vacancy migration is lower than for magnesium migration, un-

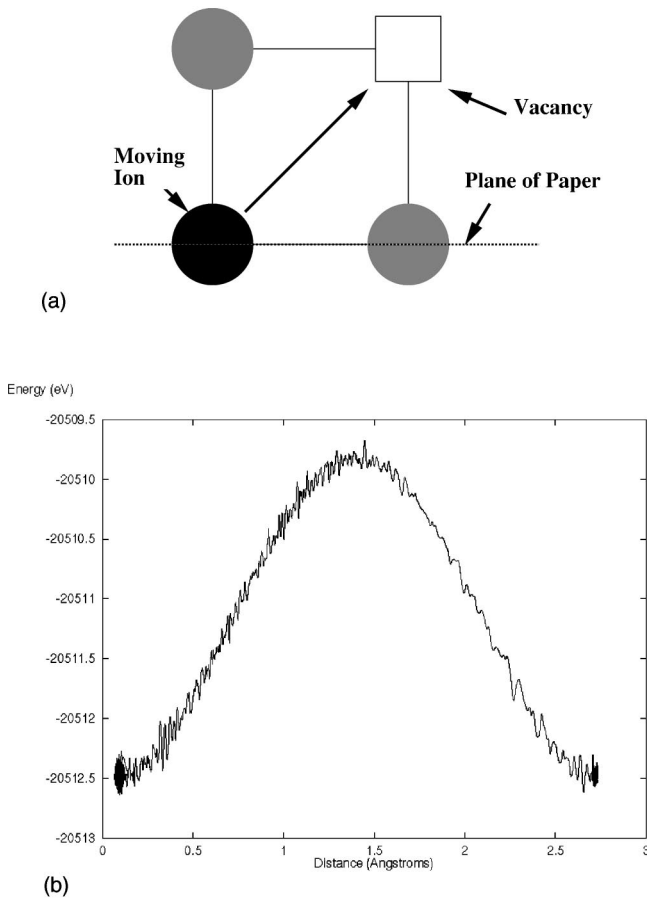


FIG. 4. (a) Schematic diagram of the diffusion pathway and (b) energy profile for vacancy migration in bulk MgO at 40 GPa, giving a guide to the magnitude in the energy fluctuations as the ion migrates to an adjacent vacant site.

like at 0 GPa. The ion followed a linear pathway between the starting and finishing sites, as shown in Fig. 4(a). The energy plot for magnesium is given in Fig. 4(b).

The diffusion pathways and migration energies were then considered for the 40 GPa grain boundary. The migration energies and directions of travel for magnesium vacancies are given in Fig. 5(a) for 40 GPa compared to the 0 GPa values in Fig. 5(b). Two types of diffusion are discussed in the following sections, along the grain boundary and down the dislocation pipe. Again oxygen vacancy migration energies were generally slightly lower than those for magnesium at high pressure although the energies were strongly correlated. Thus in the following sections we will focus on magnesium vacancy migration as this is calculated to be the slowest migrating species and hence the most relevant to creep processes.

B. Diffusion between the dislocation pipes

Diffusion along the boundary was defined as migration from one dislocation pipe to an adjacent one whilst remaining on one side of the boundary, e.g., A to A' . For diffusion between sites A , B , C , and D the moving ion exhibited a curved trajectory that took the ion slightly into the bulk crys-

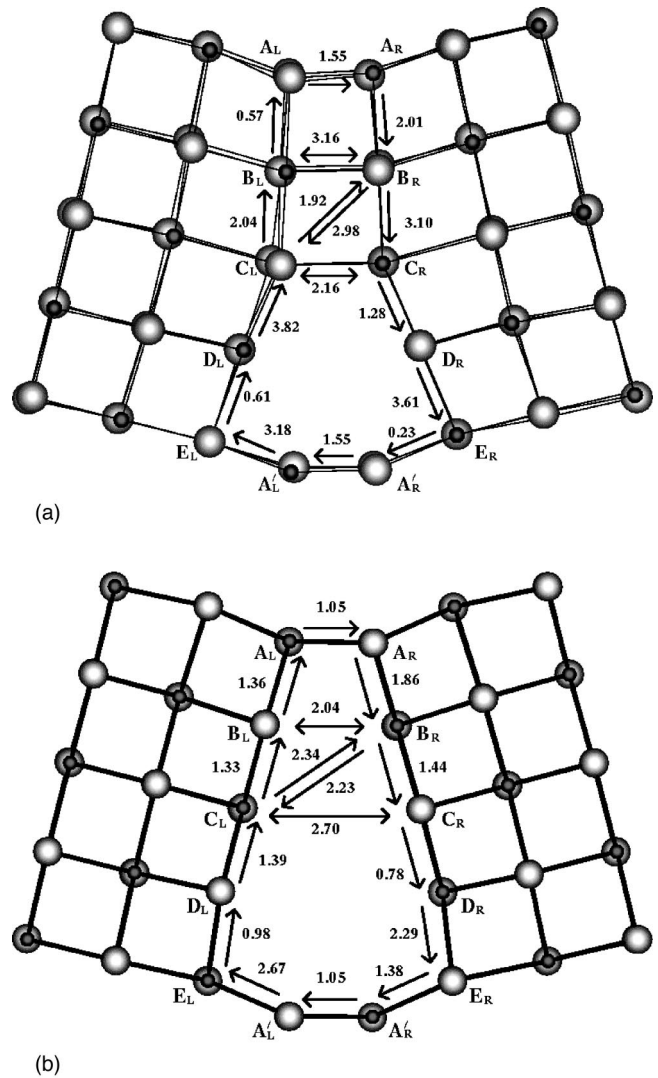


FIG. 5. The migration energies for vacancy migration of magnesium at (a) 40 GPa and (b) 0 GPa (taken from Ref. 13).

tal and away from the boundary. For example, between sites C and D , the moving ion was displaced approximately 0.3 \AA perpendicular to the main direction of travel. This may be a result of the boundary layer compressing more than the bulk. The effect of pressure caused the C sites on either side of the boundary to draw together upon compression whilst the bulk remained relatively static, leaving an enlarged space on the bulk side of the boundary ions for the ions to migrate. The rate-determining step for migration between the dislocation pipes was for magnesium between sites D and C with an energy of $3.82 \pm 0.1 \text{ eV}$. In comparison, at 0 GPa the rate-determining step was between sites D and E with an migration energy of $2.29 \pm 0.1 \text{ eV}$ for magnesium and oxygen. At 40 GPa the energies of diffusion to the unstable E site were high; however, as previously described, a vacancy initially at the D position was stabilized by the movement of the ion at A' to a point between the two sites. This means that diffusion would bypass the E site. In contrast to that at 0 GPa where the more open structure of the boundary prevents this and the vacancy would become bound at site D .

C. Diffusion down the dislocation pipes

Diffusion down the boundary was defined as migration within a single dislocation pipe and occurs when the ion crosses the boundary to the opposite face, e.g., A_L to A_R or B_L to B_R . The route A_L to A_R was the preferred with a migration energy of 1.55 ± 0.1 eV for magnesium vacancy migration compared to the bulk value of 2.68 ± 0.1 eV. At 0 GPa the migration energy for magnesium vacancy migration was 1.05 ± 0.1 eV compared to 1.94 ± 0.1 eV for bulk. The moving ion did not significantly enter the dislocation core for this diffusion pathway.

One interesting point concerned diffusion down the boundary between sites B and C , which can proceed either along one side of the dislocation or it can hop from one side of the boundary to other. At low pressures movement across the boundary is unlikely because of the distance and energy barrier. But at high pressures the collapse of the grain boundary now makes transport from one side of the boundary to the other the preferred pathway at high pressure. Although only speculation at this stage, it may have consequences for grain growth via movement of the boundary.

The migration energies for diffusion down the cores were 0.12 eV lower than those for diffusion between the cores. In both cases diffusion away from the C site is preferred to diffusion to this site. As noted earlier, an ion traveling between the pipes from site B_L to C_L followed a curved trajectory that takes it slightly into the bulk. In contrast, an ion traveling down the pipes from site B_L to C_R followed a linear route. This ion traveled a shorter distance and thus could contribute to a higher diffusion coefficient.

D. The concentration and mobility of bound defects

The calculations presented suggest that the enhanced diffusion rates at the grain boundary are a result of the lower migration energies and increased free vacancy concentrations. This agrees with the suggestion by Meyer et al.¹² who performed a MD study in the $\{310\}/[001]$ NiO tilt grain boundary under ambient pressures. The similar energies of formation of the magnesium and oxygen vacancies suggest that there will be equal concentrations of cation and anion vacancies at the boundary. This coupled with the low formation energy relative to the bulk means that there is a greater likelihood that bound vacancies will occur at high pressure. We have therefore calculated the relative concentration of bound pairs at the boundary relative to isolated vacancies in the bulk using the method described earlier. The Schottky defect energies for a bound pair at site A in the boundary were calculated as 0.19 eV at 40 GPa, compared to 5.49 eV at 0 GPa. This resulted in a boundary to bulk defect concentration ratio of 2.57×10^{15} at 40 GPa compared with 6.30×10^5 at 0 GPa, much higher than those calculated for isolated vacancies at the boundary. The binding energies of the vacancy pairs in our calculation are high, 4.83 eV, suggesting that the vacancies would prefer to remain bound. Thus under high pressures, for example, those experienced in the Earth's mantle, the defect concentration will be high and the rate-determining step for a vacancy migrating along the boundary may be the separation of the bound pair. We performed cal-

culations to evaluate the migration energy of one vacancy in a bound pair moving along the route from A_L to A_R to the next-nearest-neighbor position. The simulations showed that when an ion was forced to move to an adjacent vacant site the neighboring oppositely charged ion moved with it, resulting in the vacancies remaining bound during the diffusion process. The migration energy for the ion pair move was calculated to be 2.49 ± 0.1 eV compared to 2.68 ± 0.1 eV for bulk magnesium single-vacancy migration and 2.58 ± 0.1 eV for bulk oxygen single-vacancy migration. At 0 GPa the migration energy for single magnesium and oxygen vacancy migration down the dislocation pipe is 2.12 ± 0.1 eV. Although the vacancies do not migrate as a bound pair under ambient pressures, the presence of a nearby oppositely charged vacancy does modify the migration energy. The effect is to increase the migration energy so that it approaches that of the bulk, i.e., 1.87 ± 0.1 eV compared to the bulk values of 1.94 ± 0.1 eV. Thus the simulations predict that at higher pressures the major diffusing species along the boundary will be the charge neutral vacancy pairs.

IV. CONCLUSIONS

The effect of pressure on the defect partial Schottky energies and vacancy migration pathways has been calculated for MgO. At high pressure magnesium rather than oxygen vacancies have the highest migration energies, in contrast to the case at ambient pressures. Given the potential errors associated with using the rigid ion potential, small changes in the activation energies should not be overinterpreted. However, the change in the relative migration energies of oxygen and magnesium with pressure does seem to be a small but real effect. The reason is related to the difference in volume of the defect activated state compared to the volume of the defect on a lattice site; thus the defect with the largest difference in volume will have to do more work to migrate. The crossover occurs because the stability and defect volume of magnesium and oxygen vacancies vary differently with pressure.²³

We found that thermally generated vacancy concentrations were higher at the boundary than within the bulk and that this relative concentration increased as the pressure was increased due to the vacancy sites in the boundary becoming even more stable relative to the bulk. At high pressure a vacancy at the lowest energy site caused the formation of a structure in which a neighboring ion moved to a position midway between the two sites allowing a short-circuit for diffusion.

Diffusion for isolated magnesium and oxygen vacancy hopping down dislocation pipes forming the grain boundary was found to have a lower migration energy than that for bulk diffusion. However, the low boundary vacancy energies suggest that there will be high vacancy concentrations at the boundary and that they will be bound. Pressure increases the concentration and likelihood of bound vacancies. At 40 GPa these vacancies remained bound during diffusion resulting in a migration energy that was similar to that of bulk. The low

vacancy energies also suggest that the boundary would be a barrier to diffusion through bulk material since the segregation energy would favor vacancies remaining at the boundary. Diffusion would thus occur preferentially along the boundary.

Finally, in the future we intend to consider the effect of impurities, which may have an impact on the diffusion pro-

cess and consider the diffusion processes in other materials, for example, the mantle-forming silicate phases.

ACKNOWLEDGMENTS

We would like to thank the NERC (GR3/11779) for funding this work and MSI for the provision of their Insight II program.

*Address for correspondence.

- ¹A. G. Crouch and J. Robertson, *Acta Metall. Mater.* **38**, 2567 (1990).
- ²M. Backhausricoult and A. Peyrotchabrol, *Philos. Mag. A* **73**, 973 (1996).
- ³T. Kizuka, M. Iijima, and N. Tanaka, *Mater. Sci. Forum* **233**, 405 (1997).
- ⁴I. Yasuda, K. Ogasawara, and M. Hishinuma, *J. Am. Ceram. Soc.* **80**, 3009 (1997).
- ⁵A. Atkinson and R. I. Taylor, *Philos. Mag. A* **43**, 979 (1981).
- ⁶A. Atkinson, A. E. Hughes, and A. Hammou, *Philos. Mag. A* **43**, 1071 (1981).
- ⁷B. J. Wuensch and H. L. Tuller, *J. Phys. Chem. Solids* **55**, 975 (1994).
- ⁸W. Lojkowski, U. Södervall, S. Mayer, and W. Gust, *Interface Sci.* **6**, 187 (1998).
- ⁹V. S. Stubican and L. R. Carinci, *Z. Phys. Chem. (Munich)* **207**, 215 (1998).
- ¹⁰J. H. Harding and C. Noguera, *Philos. Mag. Lett.* **77**, 315 (1998).
- ¹¹D. M. Duffy and P. W. Tasker, *Philos. Mag. A* **54**, 759 (1986).
- ¹²M. Meyer, T. Karakasidis, and C. Waldburger, *Mater. Sci. Forum* **207-209**, 525 (1996).
- ¹³D. J. Harris, G. W. Watson, and S. C. Parker, *Phys. Rev. B* **56**, 11 477 (1997).
- ¹⁴D. J. Harris, G. W. Watson, and S. C. Parker, *Philos. Mag. A* **74**, 407 (1996).
- ¹⁵D. J. Harris, G. W. Watson, and S. C. Parker, *Am. Mineral.* **84**, 138 (1999).
- ¹⁶G. V. Lewis and C. R. A. Catlow, *J. Phys. C* **18**, 1149 (1985).
- ¹⁷B. G. Dick and A. W. Overhauser, *Phys. Rev.* **112**, 90 (1958).
- ¹⁸W. G. Hoover, *Phys. Rev. A* **31**, 1695 (1985).
- ¹⁹S. Nosé, *J. Phys.: Condens. Matter* **2**, SA115 (1990).
- ²⁰C. W. Gear, *Numerical Initial Value Problems in Ordinary Differential Equations* (Prentice-Hall, Englewood Cliffs, NJ, 1986).
- ²¹G. W. Watson, S. C. Parker, and A. Wall, *J. Phys.: Condens. Matter* **4**, 2097 (1992).
- ²²G. W. Watson, A. Wall, and S. C. Parker, *Phys. Earth Planet. Inter.* **89**, 137 (1995).
- ²³G. W. Watson, S. C. Parker, and A. Wall, *J. Phys.: Condens. Matter* **12**, 8427 (2000).
- ²⁴L. Vocadlo, A. Wall, S. C. Parker, and G. D. Price, *Phys. Earth Planet. Inter.* **88**, 193 (1995).
- ²⁵D. M. Duffy and P. W. Tasker, *Philos. Mag. A* **50**, 143 (1984).